

SWS spectroscopy of small grain features across the M17-Southwest photodissociation front^{*}

L. Verstraete¹, J.L. Puget¹, E. Falgarone², S. Drapatz³, C.M. Wright³, and R. Timmermann³

¹ Institut d'Astrophysique Spatiale, Université Paris-Sud, Bât.121, F-91405 Orsay, France

² Radioastronomie millimétrique, Ecole Normale Supérieure, 24 rue Lhomond, F-75005 Paris, France

³ Max Planck Institut für extraterrestrische Physik, Postfach 1603, D-85740 Garching, Germany

Received 15 July 1996 / Accepted 30 August 1996

Abstract. We present SWS spectra taken across the M17-Southwest photodissociation front and discuss spectral properties of PAHs and VSGs. We report new features at 4.65, 6.35, 8.7 and 11 μm which we interpret as PAHs and/or VSGs emission. From feature intensity ratios along the cut, we find PAHs are mainly ionized and almost fully hydrogenated.

Key words: ISM: molecules – ISM: dust – ISM: molecular cloud, HII region

1. Introduction

M17SW is a region where young, massive stars shine on a dense molecular complex. It is bright (total IR luminosity of 6 to 7 $10^6 L_{\odot}$, Wilson *et al.* 1979) and situated 2.2 kpc away from the sun (Chini *et al.* 1980). The photodissociation front has a fairly well defined edge-on geometry (Stutzki *et al.* 1988). Both the HII region and the molecular cloud have been recognized inhomogeneous (Felli *et al.* 1984, Stutzki & Güsten 1990). The C¹⁸O maps of Stutzki & Güsten (1990) show a steep density gradient towards the molecular cloud. This copiously irradiated ridge favours the excitation of molecular and dust emission features (Bregman *et al.* 1989, Giard *et al.* 1992). The present SWS observations have been planned to investigate the physics of small grains at such interfaces and we focus on their spectroscopic signatures ($\lambda/\delta\lambda \sim 30$).

The family of dust features at 3.3, 6.2, 7.7, 8.6, 11.3 and 12.7 μm has been observed towards many bright interstellar sources over the past 15 years and polycyclic aromatic hydrocarbons (PAHs) have been proposed as the origin of this

emission (see Léger *et al.* 1989, Allamandola *et al.* 1989a for reviews). Due to their small size, PAHs emit during temperature fluctuations after single photon absorption as opposed to classical big grains. In addition, a population of very small grains (VSGs) is required to explain the IRAS emission at 25 and 60 μm (Desert *et al.* 1990) and so far the exact nature of VSGs is unclear. PAHs features are now known to be ubiquitous in the general interstellar medium (Giard *et al.* 1994, Ristorcelli *et al.* 1994 and Boulanger *et al.*, Mattila *et al.* 1996 this issue). In the PAH model, the 3.3, 8.6 and 11.3–12.7 μm features correspond to aromatic CH-stretch, in-plane and out-of-plane bending modes respectively. When there is no adjacent hydrogen atom on the aromatic ring the CH-out-of-plane mode falls at 11.3 μm (solo mode); it shifts to around 12 (12.7) μm when there are 1 (2) adjacent hydrogen atoms (duo and trio modes, see above quoted reviews). The bands at 6.2 and 7.7 μm involve skeleton CC-modes of PAHs.

2. Data reduction

The data presented here is part of the guaranteed-time central program MPEWARM performed by the Short Wavelength Spectrometer (SWS) on board the ISO satellite (de Graauw *et al.*, Kessler *et al.* 1996 this issue). SWS-AOT1 complete spectra (2.4–45 μm , scanspeed 2) have been taken along a 3.5 arcminutes northeast-southwest cut (from RA=18h17m35.9s, Dec=-16°13'14" to RA=18h17m23.4s, Dec=-16°14'44", 1950 equinox) identical to that of Stutzki *et al.* (1988). In 10 equally spaced positions (labeled 1 to 10, first position in the HII region), one goes from the HII region towards the molecular cloud. Standard data reduction has been performed at MPE during 6 to 8th of May 1996. All the data presented here has been rebinned to a resolving power of 300. Mean relative error was around 30, 20, 10 and 5% in bands 1, 2, 3 and 4 respectively. At this rapid scanspeed narrow ($\lambda/\delta\lambda \geq 500$), bright lines were confused with glitches and removed; we retrieved them from the raw data. The 2c/3a-band match of continua was poor (fig.2a): between 12.5 and 14 μm the 3a-band curves up with decreasing

Send offprint requests to: L. Verstraete (verstra@ias.fr)

^{*} Based on observations with ISO, an ESA project with instruments funded by ESA Member States (especially the PI countries: France Germany, the Netherlands and the United Kingdom) and with the participation of ISAS and NASA.

wavelength, lying above the 2c-band by less than 30%. While re-binning, however, the weight of the 3a-band around $12.5\mu\text{m}$ was low enough not to introduce any spurious feature. To increase the signal-to-noise ratio, we averaged data taken at positions which showed similar spectral behaviour: the "HII-region" and "Interface" spectra group 3 positions each (1-2-3 and 4-5-6 respectively), the "Molecular cloud" spectrum sums up the 4 last positions. In summary, small grain features are often seen with high signal-to-noise ratios in spectral regions where calibration errors are estimated to be less than 20% (Schaeidt *et al.* 1996, this issue).

3. Spectral analysis

Spectra are given in fig.1 & 2. In the HII region, recombination and fine structure lines dominate the spectrum. In the other spectra, dust features are prominent. Concentrating on small grain features, we restrict ourselves to the $2.4\text{--}14\mu\text{m}$ range; the analysis of the remaining data will be done in a forthcoming paper. The continuum could be uncertain by significant factors when signal is weak. These systematic effects are very clear in fig.1c below $4\mu\text{m}$; yet they do not affect the intensity of dust features we are dealing with. In fig.1a, the continuum rises below $4\mu\text{m}$ as expected from emission of the ionized gas in the HII region. PAH features are present in the 3 spectra. The $3.3\mu\text{m}$ band extends to a plateau at longer wavelengths and the $3.4\mu\text{m}$ -feature is clearly visible in figs.1b&c. The latter has been assigned to the aliphatic CH-stretch of methyl side groups on PAHs (de Muizon *et al.* 1986, Shan *et al.* 1991, Joblin *et al.* 1996). The emission plateau may arise from hot bands, overtone and combination modes (Allamandola *et al.* 1989b, Geballe *et al.* 1989) or anharmonic vibrational progression (Talbi *et al.* 1993). In the HII region, the $\text{Pf}\delta$ [$3.296\mu\text{m}$] line falls within the $3.3\mu\text{m}$ -band (fig.1a): we subtracted its intensity assuming it is a tenth of the $\text{Br}\alpha$ [$4.05\mu\text{m}$] line (Hummer & Storey 1987). Other features are detected at 4.65 , 5.25 and $5.65\mu\text{m}$ at the interface with a signal-to-noise ratio of at least 15. The two latter bands have been ascribed to PAH combination modes (Allamandola *et al.* 1989b, Roche *et al.* 1996). The $4.65\mu\text{m}$ -band, very similar, is to our knowledge unreported so far and could have the same origin (it is also seen in the HII region with the $\text{Pf}\beta$ [$4.654\mu\text{m}$] and possibly a HeI recombination line superimposed).

The $8.6\mu\text{m}$ feature changes dramatically in the HII region: it broadens, gets stronger than the $7.7\mu\text{m}$ and shifts towards $8.7\mu\text{m}$. In addition, the $6.2\text{--}7.7\text{--}8.7\mu\text{m}$ features sit on top of a broad continuum extending from 6 to $11\mu\text{m}$. We also find two new features at $6.35\mu\text{m}$ (a red shoulder of the $6.2\mu\text{m}$ -band, note the superimposed $[\text{ArIII}]6.37\mu\text{m}$ line) and $11\mu\text{m}$ in the HII region (the latter is also present in the other spectra). The $7.7\mu\text{m}$ -band has 2 peaks (figs.2c&d) at 7.6 and $7.8\mu\text{m}$. Recent work (Langhoff 1996 and references therein) shows that the 6.2 and 7.7 , $11.3\mu\text{m}$ bands shifts to longer and shorter wavelengths respectively when PAHs are singly ionized. Hence, our spectra suggests that PAHs are mainly ionized. A similar modification of the PAH emission spectrum has been seen towards compact HII regions (Roelfsema *et al.* 1996, this issue). Away from the

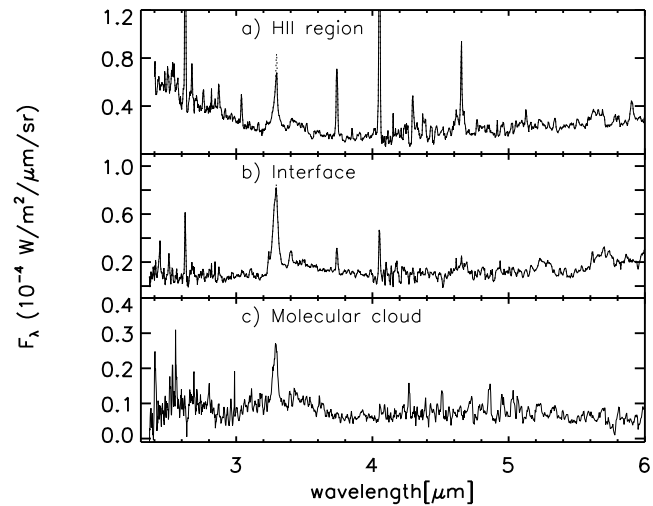


Fig. 1. SWS-AOT1 spectra in the $2.4\text{--}6\mu\text{m}$ range. In a) and b), the spectrum not corrected for the $\text{Pf}\delta$ line at $3.3\mu\text{m}$ is represented by the dotted line (see text).

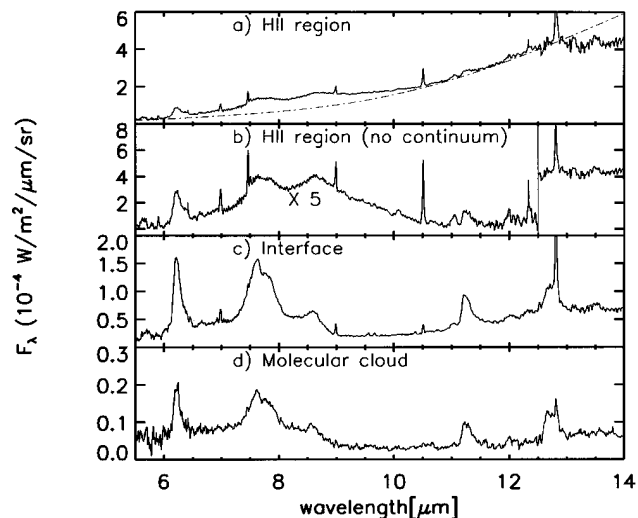


Fig. 2. Same as fig.1 for the $6\text{--}14\mu\text{m}$ range. In b), the HII region continuum (sum of two blackbodies at 120 and 280K , see the dot-dashed line in fig.2a) has been subtracted and the spectrum multiplied by 5 at wavelengths below $12.5\mu\text{m}$.

HII region, spectra exhibit a band at $12\mu\text{m}$ probably due to the duo CH-modes of PAHs (see also Cesarsky *et al.* 1996). The $12.7\mu\text{m}$ -feature would then correspond to the trio CH-mode (the $\text{NeII}[12.81\mu\text{m}]$ is superimposed). Similar bands have been detected in the past at lower resolution (Roche *et al.* 1989, Cohen *et al.* 1985). Two more features at 13.1 and $13.5\mu\text{m}$ appear in all spectra (see §4).

4. The physical state of PAHs across the M17-photodissociation front

From our spectra we have derived band intensities at all positions by simply subtracting a straight baseline at the bottom of

each band. Thus, continuum uncertainties (see §2&3) do not affect our band intensities. The 6.2, 7.7 and 8.6 μm bands sit on top of a broad plateau which may be related to PAHs (Bregman *et al.* 1989, Boulanger *et al.* 1996): we have, however, taken only the narrow bands and not this underlying broad feature to estimate intensities. In the HII region, systematic errors prohibited a reliable estimate of the 12.7 μm intensity. At other positions, we estimate the error on the 12.7 μm -band intensity due to the poor 2c/3a band match (see §2) to be within the error bar. All PAH feature profiles (fig.3) peak at the interface: such a limb brightening effect has been observed in other regions and can only be understood if the PAH abundance varies (see *e.g.*, Bregman *et al.* 1989, Bernard *et al.* 1993). Conversely, the 16 μm -continuum decreases monotonously away from the second position. The 3.3, 11.3 μm and the CC-modes profiles are very similar (our mean 6.2/7.7 ratio is 0.5). The 12 and 12.7 μm profiles are slightly offset towards the molecular cloud with respect to the 11.3 μm suggesting that PAHs rehydrogenate in shielded regions. The 6.35 μm feature vanishes rapidly away from position 1. All these features are decorrelated from the 16 μm -continuum, a behaviour characteristic of single photon heating which supports the PAH hypothesis. In the HII region, the 8.7 and 11 μm intensities follow the 16 μm -continuum suggesting they originate mainly from VSGs which dominate the continuum at these wavelengths (Désert *et al.* 1990). Towards the molecular cloud the 8.6 and 11 μm emission, in excess of the 16 μm -continuum, is mainly due to PAH cations (see below). The 13.1 and 13.5 μm -bands correlate with the 16 μm -continuum throughout the cut. Artefact arising from ill-calibrated data could produce such features and we plan to inquire again this spectral region. A comparable 13.5 μm -feature appears in ISOCAM-CVF spectra (Cesarsky *et al.* 1996). If real these features, correlated to continuum, would again be the signature of VSGs emission.

At the interface and in the HII region, PAHs are exposed to a harder radiation field: they can be ionized, loose hydrogen atoms and/or disappear by photodissociation. We define below band ratios able to trace these events. The effect of single ionization (Szczepanski & Vala 1993, DeFrees *et al.* 1993, Hudgins & Allamandola 1995, Langhoff 1996) on the infrared modes of PAHs has recently been investigated. So far only small PAHs are involved whereas interstellar PAHs are probably larger (Désert *et al.* 1990): we assume the above results also hold for larger species. Clear trends appear when comparing the spectra of PAH cations with neutrals (Langhoff 1996). Ionization depresses the 3.3 μm band by factors of 10 to 100 (the spread is large between laboratory measurements and also with theoretical results); conversely the 6.2, 7.7 and 8.6 μm bands are larger in cations by at least a factor 10. These changes are best traced with band ratios. The ratio of in-plane CC to CH-out-of-plane modes (6.2 + 7.7)/(11 to 13) is about 0.4 for neutral PAHs vs 4 for cations, we note this ratio ION and use it as a tracer of PAH ionization.

The ION profile is shown on fig.3. At the 3 first positions, the 12.7 μm -intensity was not available: we estimated an upper limit by taking the 12.7 μm and 11.3 μm intensities equal and a lower limit with the 12.7 μm intensity set to zero. Our ION ratio varies between 2 (molecular cloud and lower limit in the

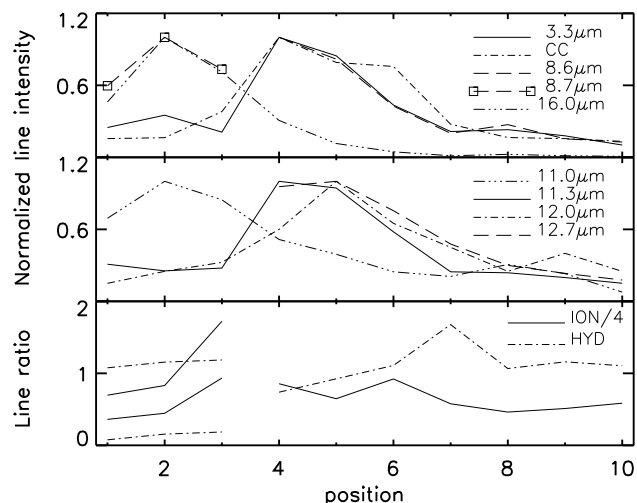


Fig. 3. Profiles across our M17SW cut. Abscissae are position numbers, the distance between 2 subsequent positions is 23.3 arcseconds. **Top and middle:** PAH band intensity profiles. Ordinates are normalized to peak values (in $10^{-6} \text{W m}^{-2} \text{sr}^{-1}$): 4.9(3.3 μm), 94(CC=6.2+7.7 μm), 14(8.6 μm), 13.6(8.7 μm), 16(11.3 μm), 1.9(12 μm), 11.2(12.7 μm) and $6.5 \cdot 10^{-4} \text{W m}^{-2} \mu\text{m}^{-1} \text{sr}^{-1}$ (16 μm -continuum). **Bottom:** band intensity ratios (see text). The ION ratio has been divided by 4. At the 3 first positions, only upper and lower limits to ION and HYD are given (see text).

HII region) and 3.3 (interface). Adopting the intrinsic band ratios quoted above, these values correspond to a PAH ionized fraction of 44 and 80% respectively. We have so far assumed that the same species emits in all the PAH features. However, in a given radiation field, an interstellar PAH emits at a color temperature fixed by its size and the smaller (larger) species dominate the emission at short (long) wavelengths. Using the Désert *et al.* (1990) model, we estimated this color variation effect to enhance ION by a factor 1.7 with respect to its value for a single PAH: this reduces our ionized fractions to 22 and 43%. The latter value is a lower limit: indeed, in the HII region and at the interface the smallest PAHs are expected to be photodissociated (Allain *et al.* 1996) so that color temperature variations should be smaller because of the smaller size range. Final numbers will be obtained from detailed modelling of the complete infrared spectrum involving emissivities of PAH cations and taking into account PAH destruction. PAHs would thus be mainly ionized in the HII region and interface and mostly neutral in the molecular cloud. The 6.35 μm -band, strongest in the HII region, could thus be due to large ionized PAHs which can survive in the strong radiation field. Dehydrogenation has a less dramatic influence than ionization (Pauzat *et al.* 1995). The CC-modes remain unchanged in the neutral and cation while the CH-out-of-plane modes vary proportionately to the hydrogen coverage. The 2 other modes (3.3 and 8.6) have opposite behaviour for the neutral and ion. To trace PAH dehydrogenation independently of ionization, we define the ratio $\text{HYD} = (12 + 12.7)/11.3$ which rises as PAH rehydrogenate (Schutte *et al.* 1993). From position 4 to 10 this ratio increases from 0.8 to 1.2 (fig.3). As for ION

we calculated an upper and a lower limit for HYD in the HII region, they are 1.2 and 0.2 respectively. Assuming PAHs are fully hydrogenated in the molecular cloud, we find a degree of hydrogenation of 80% at the interface and of at least 40% in the HII region. Spectra of the Orion bar (Bregman *et al.* 1989, Roche *et al.* 1989) yield very similar values of ION and HYD. Finally, our mean 3.4/3.3 intensity ratio is about 0.1 implying a radiation field of 10^5 times standard (Joblin *et al.* 1996) consistent with earlier work (Stutzki *et al.* 1988, Giard *et al.* 1992). In the molecular region, the feature emission would thus occur in the unshielded outer parts of dense clumps.

5. Conclusions

We have studied the evolution of small grain dust features across the M17SW photodissociation region with SWS-AOT1 spectra. Intensity profiles of PAH features peak at the interface as expected in a picture where PAHs are destroyed in the HII region and condense in molecular regions. We have defined line ratios tracing the fraction of PAH cations as well as their degree of hydrogenation. PAHs are mainly ionized at the interface and in the HII region. PAHs probably have a high hydrogenation degree increasing towards the molecular cloud. We report new bands at 4.65, 6.35, 8.7, 11 μm and confirm the presence of the 12 μm duo CH-mode of PAHs. In the HII region the (broad) 8.7 and 11 μm bands, correlated with the mid-infrared continuum, could be the signature of VSGs emission.

Acknowledgements. We thank D. Lutz, E. Wieprecht and all the ISO team at MPE for their help with data reduction. We are grateful to our referee, Xander Tielens, who made many useful comments.

References

- Allain, T., Leach, S., Sedlmayr, E., 1996: A&A 305,602 and 616
 Allamandola, L.J., Tielens, A.G.G.M., Barker, J.R., 1989: ApJS 71,733
 Allamandola, L.J., Bregman, J.D., Sandford, S.A., Tielens, A.G.G.M., Witteborn, F.C., Wooden, D.H., Rank, D., 1989: ApJ 345,L59
 Bernard, J.P., Boulanger, F., Puget, J.L., 1993: A&A 277,609
 Bregman, J.D., Allamandola, L.J., Tielens, A.G.G.M., Geballe, T.R., Witteborn, F.C., 1989: ApJ 344,791
 Chini, R., Elsässer, H., Neckel, T., 1980: A&A 91,186
 Cohen, M., Tielens, A.G.G.M., Allamandola, L.J., 1985: ApJ 299,L93
 DeFrees, D.J., Miller, M.D., Talbi, D., Pauzat, F., Ellinger, Y., 1993: ApJ 408,530
 Désert, F.X., Boulanger, F., Puget, J.L., 1990: A&A 237,215
 Felli, M., Churchwell, E., Massi, M., 1984: A&A 136,53
 Geballe, T.R., Tielens, A.G.G.M., Allamandola, L.J., Moorhouse, A., Brand, P.W.J.L., 1989: ApJ 341,278
 Giard, M., Bernard, J.P., Dennefeld, M., 1992: A&A 264,610
 Giard, M., Lamarre, J.M., Pajot, F., Serra, G., 1994: A&A 286,203
 Hudgins, D.M., Allamandola, L.J., 1995: J. Phys. Chem. 99,3033
 Hummer, D.G., Storey, P.J., 1987: MNRAS 224,801
 Joblin, C., Tielens, A.G.G.M., Allamandola, L.J., Geballe, T.R., 1996a: ApJ 458,610
 Langhoff, S.R., 1996: J. Phys. Chem. 100,2819
 Léger, A., d'Hendecourt, L., Défourneau, D., 1989: A&A 216,148
 de Muizon, M., Geballe, T.R., d'Hendecourt, L.B., Baas, F., 1986: ApJ 306,L105
 Pauzat, F., Talbi, D., Ellinger, Y., 1995: A&A 293,263
 Ristorcelli, I. *et al.*, 1996: A&A 286,L23
 Roche, P.F., Aitken, D.K., Smith, C.H., 1989: MNRAS 236,485
 Roche, P.F., Lucas, P.W., Geballe, T.R., 1996: MNRAS 281,L25
 Schutte, W.A., Tielens, A.G.G.M., Allamandola, L.J., 1993: ApJ 415,397
 Shan, J., Suto, M., Lee, L.C., 1991: ApJ 383,459
 Stutzki, J., Stacey, G.J., Genzel, R., Harris, A.I., Jaffe, D.T., Lugten, J.B., 1988: ApJ 332,379
 Stutzki, J., Güsten, R., 1990: ApJ 356,513
 Szczepanski, J., Vala, M., 1993: ApJ 414,646
 Talbi, D., Pauzat, F., Ellinger, Y., 1993: A&A 268,805
 Wilson, T.L., Fazio, G.G., Jaffe, D.T., Kleinman, D.E., Wright, E.L., Low, F.J., 1979: A&A 76,86